Spectral properties in the charge density wave phase of the half-filled Falicov-Kimball Model

S.R.Hassan[1,2], H. R. Krishnamurthy[2,*]
[1] *Département de Physique,Université de Sherbrooke, Québec, Canada J1K 2R1 and*
[2] *Centre for Condensed Matter Theory, Department of Physics, Indian Institute of Science, Bangalore 560 012, India*

We study the spectral properties of charge density wave (CDW) phase of the half-filled spinless Falicov-Kimball model within the framework of the Dynamical Mean Field Theory. We present detailed results for the spectral function in the CDW phase as function of temperature and U. We show how the proximity of the non-fermi liquid phase affects the CDW phase, and show that there is a region in the phase diagram where we get a CDW phase without a gap in the spectral function. This is a radical deviation from the mean-field prediction where the gap is proportional to the order parameter.

I. INTRODUCTION

Metzner and Vollhardt[1] pioneered a new approach to the study of strongly correlated electron systems which is exact in the limit of infinite dimensionality. Generally referred to as Dynamical Mean-Field Theory (DMFT), the method has been developed further in the subsequent years and has led to substantial progress in our understanding of these systems[2,3]. Soon after the work of Metzner and Vollhardt[1], in a series of papers[4], Brandt and Mielsch showed that the large dimensional limit of the spin-less Falicov-Kimball model (SFKM)[5] is exactly soluble and studied various aspects of the solution. One of the first issues examined in the SFKM using the DMFT was that of ordering into a two sublattice, "checkerboard", charge density wave (CDW) state that is expected to arise in the model at half-filling on a hyper cubic lattice. Because the hyper cubic lattice is bipartite, a transition at a non-zero temperature is expected[6] for all U and indeed this is true within the DMFT as well[4].

Since the original work[4], a number of other studies of the 'uniform phase' at high temperatures, the CDW order and of phase separation away from half filling have followed[7,8,9,10,11,12], on both the hyper cubic and Bethe lattices. The homogeneous or uniform phase at high temperatures is a non-Fermi liquid[7]. A detailed study of transport in this phase has been carried out by Moller *et al*[8]. Van dongen[9] pointed out that for a lattice with a bounded density of states (DOS) the half-filled system in the uniform phase displays a metal-insulator transition at a non-zero U. Since the DMFT is in the thermodynamic limit, one can determine the transition temperature for the continuous transition from the uniform to the CDW phase simply by finding the temperature at which the charge susceptibility at wave-vector $\vec{Q}_0 \equiv (\pi, \pi, ...)$ diverges. Thus one can obtain the phase diagram of the half filled system purely from the knowledge of the uniform solution. The phase diagram for commensurate and incommensurate filling (away from half filling) in one and two dimensions within the frame work of the DMFT has been studied by Freericks[10].

Despite all this work, the properties of the CDW phase itself do not seem to have been explored a great deal. In this contribution, we study the spectral and transport properties of the charge density wave (CDW) phase of the half-filled SFKM in the DMFT approximation at a level of detail not reported before, to the best of our knowledge. We present detailed results for the spectral functions in the CDW phase as functions of temperature and U. We show how the non-Fermi liquid behavior in the uniform phase affects the CDW phase, and show that there is a region in the phase diagram, not emphasized in the literature before, where we get a CDW phase without a gap in the spectral function. This is a radical deviation from the static mean-field prediction where the gap is proportional to the order parameter, and the CDW phase is always gapped. The 'transition temperature' $T_l(U)$ between this novel gapless 'phase' and the conventional gapped CDW phase has an interesting 'reentrant' structure as U increases.

II. DMFT OF SFKM; FORMALISM

The Hamiltonian for the SFKM on a lattice with sites labeled by i can be written as

$$H = -\sum_{i,j} t_{ij} b_i^\dagger b_j + \epsilon_\ell \sum_i \ell_i^\dagger \ell_i - \mu \sum_i (b_i^\dagger b_i + \ell_i^\dagger \ell_i) + U \sum_i b_i^\dagger b_i \ell_i^\dagger \ell_i. \quad (2.1)$$

It includes spin-less conduction or band electrons b with hopping parameters t_{ij}, which, in this paper, we assume to be non zero only for nearest neighbors, and localized ℓ electrons conserved at each site with site energy ϵ_ℓ. μ is the chemical potential for the b and ℓ electrons. There is an on-site coulomb repulsion U between b and ℓ. In this paper, we confine ourselves to the particle hole symmetric case, with $N^{-1}\sum_i \bar{n}_{\ell i} \equiv N^{-1}\sum_i < n_{\ell i} >= 1/2$ *and* $N^{-1}\sum_i \bar{n}_{bi} \equiv N^{-1}\sum_i < n_{bi} >= 1/2$ where N is the total number of sites in the lattice. On bipartite lattices this is achieved by the choice $\epsilon_\ell = 0$, $\mu = \frac{U}{2}$.

The exact solubility of the SFKM within the DMFT approximation arises as follows[4]. In infinite dimensions, or in finite dimensions within the DMFT, the self energy, irreducible vertex functions etc., are purely local, and in diagrammatic perturbation theory, for example, are given by sums of skeleton graphs involving only the local Green's function. The problem is hence mapped to a single site or impurity problem embedded in a self consistent medium representing all the other sites of the lattice. In a functional integral formalism, the resulting single site effective action at site i is given by[2,3]

$$\mathcal{S}_{eff} = -\int_0^\beta \int_0^\beta d\tau d\tau' b_i^\dagger(\tau) {\mathcal{G}^{ii}}^{-1}(\tau-\tau') b_i(\tau') - \beta\mu n_{\ell i} + Un_{\ell i}\int_0^\beta d\tau b_i^\dagger(\tau) b_i(\tau) \quad (2.2)$$

Here $b_i^\dagger(\tau)$ and $b_i(\tau)$ are fluctuating fermionic Grassmann fields corresponding to coherent states of the b electrons, and $n_{\ell i} = 1$ or 0 corresponding to the ℓ state at site i being occupied or not. $\mathcal{G}^{ii}(\tau)$ is the bare on site local propagator (also referred to as the host or medium propagator) for the self consistent single site problem. It is essentially the local propagator at site i excluding the self energy processes at that site (since they will be recovered by solving the single site problem) but including the self energy processes at all the other sites of the lattice in some average way. (Site indices are being kept track of in the equations above with a view to using them in contexts involving broken symmetry solutions such as the CDW phase.)

Since the effective action eq. (2.2) is quadratic in the variable b for a fixed $n_{i\ell}$, the local Green's function can be calculated exactly for an arbitrary host Green's function as

$$G_n^{ii} = \frac{\mathrm{w}_{0i}}{(\mathcal{G}_n^{ii})^{-1}} + \frac{\mathrm{w}_{1i}}{(\mathcal{G}_n^{ii})^{-1} - U}\,. \quad (2.3)$$

Here $G_n^{ii} \equiv G^{ii}(i\omega_n)$ (and similarly for $\mathcal{G}$, etc.), $i\omega_n \equiv i(2n+1)\pi T$ are the Fermionic Matsubara frequencies, and w_{1i} and $\mathrm{w}_{0i} = (1 - \mathrm{w}_{1i})$ are the annealed probabilities for the ℓ state at site i being occupied and empty respectively. w_{1i}, also equal to the average ℓ electron number at site i, can be calculated as

$$\mathrm{w}_{1i} = \bar{n}_{\ell i} = \frac{Z_{1i}}{Z_{0i} + Z_{1i}}, \quad (2.4)$$

in terms of Z_{1i} and Z_{0i}, the constrained partition functions obtained by summing $\exp(-S_{eff})$ over all the fluctuating b configurations for fixed $n_{\ell i} = 1$ or 0 respectively. It is straightforward to verify that

$$Z_{\nu i} = \exp\left[\beta\mu\delta_{\nu 1} + \sum_n \ln\left(U\delta_{\nu 1} - (\mathcal{G}_n^{ii})^{-1}\right) e^{i\omega_n 0^+}\right]. \quad (2.5)$$

A renormalized or effective ℓ electron energy at site i can be defined by expressing w_{1i} as $n_F^-(\epsilon_{\ell_i}^* - \mu)$, whence

$$\epsilon_{\ell_i}^* = \mu + Tln(\frac{Z_{0i}}{Z_{1i}}). \quad (2.6)$$

The local Green's function G_n^{ii}, host Green's function $\mathcal{G}_n^{ii}$ and self energy Σ_n^{ii} are related by the local Dyson equation,

$$(G_n^{ii})^{-1} = (\mathcal{G}_n^{ii})^{-1} - \Sigma_n^{ii}. \quad (2.7)$$

Using this equation in reverse, in the form,

$$(\mathcal{G}_n^{ii})^{-1} = \Sigma_n^{ii} + (G_n^{ii})^{-1}, \quad (2.8)$$

substituting into eq. (2.3), and cross-multiplying, one gets[4] a quadratic equation which can be solved to express the self energy directly in terms of the local Green's function and w_{1i}. The result is

$$\Sigma_n^{ii} = \frac{U}{2} - \frac{1}{2G_n^{ii}}\left(1 - \sqrt{1 + (UG_n^{ii})^2 + 4(\Delta \mathrm{w}_{1i})UG_n^{ii}}\right), \quad (2.9)$$

where we have introduced

$$\Delta \mathrm{w}_i \equiv (\mathrm{w}_{1i} - \frac{1}{2}) = (\frac{1}{2} - \mathrm{w}_{0i}). \quad (2.10)$$

(The sign of the root chosen in writing eq. (2.9) is so as to reproduce the known analyticity properties of the self energy.) In terms of the ratio $x_i \equiv Z_{1i}/Z_{0i}$ which can be calculated, using eq. (2.5), as

$$x_i = \exp\left[\beta\mu + \sum_n \ln\left(\frac{(\mathcal{G}_n^{ii})^{-1} - U}{(\mathcal{G}_n^{ii})^{-1}}\right) e^{i\omega_n 0^+}\right], \quad (2.11)$$

we can write

$$\Delta \mathrm{w}_i = \frac{1}{2}\left(\frac{x_i - 1}{x_i + 1}\right). \quad (2.12)$$

We note that, although according to eq. (2.9) Σ_n^{ii} seems to depend explicitly only on G_n^{ii} at the same Matsubara frequency, implicitly, via its dependence on Δw_i and hence on x_i, it is in general a functional of G_m^{ii} at all frequencies $i\omega_m$.

To complete the DMFT procedure, one has to next invoke the DMFT self consistency relation which determines the local Green's functions in terms of the local self energies via lattice propagators, based on treating the local self energy as a good approximation (which is exact in infinite dimensions) to the lattice self energy. For this purpose we need to use the lattice Dyson equation,

$$(i\omega_n + \mu - \Sigma_n^{ii})G_n^{ij} - \sum_l t_{il}G_n^{lj} = \delta_{ij}. \quad (2.13)$$

The properties of this relation depend very much on the phase one is interested in.

III. THE UNIFORM PHASE AND THE CDW INSTABILITY

At high temperatures the b electrons and ℓ electrons are uniformly distributed on the lattice for all electron concentrations; there is no long range order, and no broken symmetry. In this case of a homogeneous or uniform phase, w_{1i}=w_1, $\Sigma_n^{ii} = \Sigma_n$, etc.; i.e., the same for all the sites i. And at half filling, by symmetry, $w_1 = \frac{1}{2}$, so that $\Delta\ w_i = 0$. Hence Σ_n becomes a single explicit *function* of G_n given by

$$\Sigma_n = \frac{U}{2} - \frac{1}{2G_n}\left(1 - \sqrt{1 + (UG_n)^2}\right). \tag{3.1}$$

The DMFT self consistency condition eq. (2.13) is easily solved in this limit simply by fourier transforming. The lattice Green's function is

$$G_{\mathbf{k}}(i\omega_n) = (i\omega_n + \mu - \Sigma_n - \epsilon_{\mathbf{k}})^{-1}\,. \tag{3.2}$$

Hence the local Green's function is

$$\begin{aligned} G_n &\equiv G_0(i\omega_n + \mu - \Sigma_n) \\ &= \int d\epsilon\ \frac{D_0(\epsilon)}{i\omega_n + \mu - \Sigma_n - \epsilon}\,, \end{aligned} \tag{3.3}$$

where $D_0(\epsilon)$ is the bare density of states(DOS) of the band structure determined by t_{ij}. Most of the results reported in this chapter have been obtained using the semi-circular DOS (SDOS) characteristic of the Bethe lattice in infinite dimensions, for which

$$D_0(\epsilon) = \frac{1}{2\pi t^2}\sqrt{4t^2 - \epsilon^2}\ ,\ \ |\epsilon| < 2t\,, \tag{3.4}$$

whence $G_0(z)$, the complex Hilbert transform of the bare DOS, can be obtained analytically, as

$$G_0(z_n) = \frac{2}{z_n + \sqrt{z_n^2 - 4t^2}}, \tag{3.5}$$

with $z_n = i\omega_n + \mu - \Sigma_n$. We also report some results using the actual density of states for a square lattice whence $G_0(z)$ has to be evaluated numerically. We will refer to these as 2DDOS results. In either case, the local Green's function and the self energy can be obtained by self consistently solving eqns. (3.1) and (3.3).

In the uniform case at half filling the temperature completely drops out of the problem, as the ℓ occupancy probabilities are fixed by symmetry. The metal-insulator transition we alluded to above[9] hence takes place at a fixed value of U independent of temperature within the DMFT. For the SDOS case this value is $U = 2t$. The temperature dependence of the b electron DOS can be restored by including spatial fluctuations using approximations that go beyond DMFT[13].

As the temperature is lowered, the homogeneous (disordered) phase becomes unstable with respect to an ordered phase where both the b and ℓ charge densities with spatial modulations at some ordering wavevector $\mathbf{q}$ develop; i.e., $\sum_i exp(i\mathbf{q}\cdot\mathbf{R_i}) < b_i^\dagger b_i >$ and $\sum_i exp(i\mathbf{q}\cdot\mathbf{R_i}) < \ell_i^\dagger \ell_i >$ acquire nonzero values. If the transition to this ordered phase is continuous (second-order), then it occurs when the charge-susceptibility (at the ordering wave vector) diverges. The static, or zero (external) frequency b-charge-susceptibility at the ordering wave vector $\mathbf{q}$ is obtainable as the Fourier transform of the b-charge-density - b-charge-density correlation function:

$$\begin{aligned} \chi(\mathbf{q},T) &\equiv -\frac{1}{N}\sum_{j,k} e^{i\mathbf{q}\cdot(\mathbf{R}_j - \mathbf{R}_k)} \times \\ &\qquad \int_0^\beta d\tau < b_j^\dagger(\tau) b_j(\tau) b_k^\dagger(0) b_k(0) >\,, \\ &\equiv T\sum_{n=-\infty}^{\infty} \bar{\chi}_n(\mathbf{q})\,, \end{aligned} \tag{3.6}$$

Here n indexes the Matsubara frequency of the fermionic propagators that arise in a diagrammatic perturbation theory evaluation of χ. Using the generalized Dyson's equation[4] valid for two particle propagators, one can relate $\bar{\chi}_n$ to the simplest "bubble graph susceptibility" $\bar{\chi}_n^0$ in the form

$$\bar{\chi}_n(\mathbf{q}) = \bar{\chi}_n^0(\mathbf{q}) - \bar{\chi}_n^0(\mathbf{q})\sum_{m=-\infty}^{\infty} \frac{\partial\Sigma_n[G]}{\partial G_m}\bar{\chi}_m(\mathbf{q})\,, \tag{3.7}$$

where $\bar{\chi}_n^0$ is given by[4]

$$\bar{\chi}_n^0(\mathbf{q}) = -\sum_{\mathbf{k}} G_n(\mathbf{k}+\mathbf{q})G_n(\mathbf{k})\,, \tag{3.8}$$

$$= -\frac{1}{\sqrt{1-X^2}}\int_{-\infty}^{\infty} d\epsilon \frac{D_0(\epsilon)}{i\omega_n + \mu - \Sigma_n - \epsilon} \times G_0\left[\frac{i\omega_n + \mu - \Sigma_n - X\epsilon}{\sqrt{1-X^2}}\right]. \tag{3.9}$$

Here $D_0(\epsilon)$ is the bare DOS as before, and all of the wave-vector dependence occurs via the quantity

$$X(\mathbf{q}) \equiv \frac{1}{d}\sum_{j=1}^{d} cos(q_j)\,. \tag{3.10}$$

and we use

$$G_0(z) \equiv \int d\epsilon D_0(\epsilon)/(z-\epsilon) \tag{3.11}$$

to denote the complex Hilbert Transform of the bare DOS as before. Similarly, the ℓ-ℓ charge correlation function defined by

$$\chi_{\ell-\ell}(\mathbf{q},T) \equiv \frac{1}{NT}\sum_{j,k} e^{i\mathbf{q}\cdot(\mathbf{R}_j - \mathbf{R}_k)} < n_{\ell j} n_{\ell k} > \tag{3.12}$$

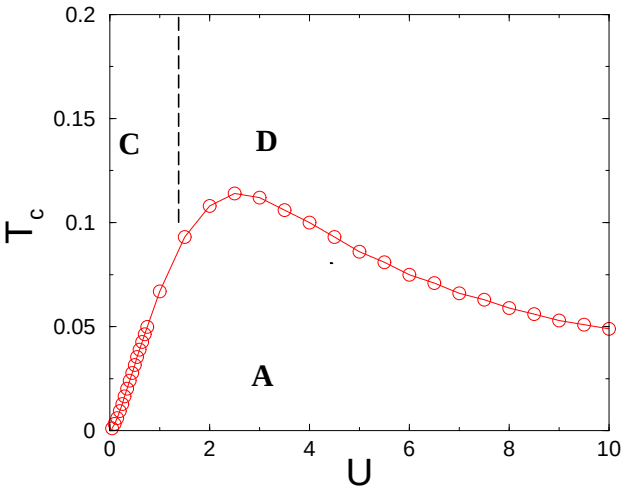

FIG. 1: (Color online)Conventional phase diagram of the half-filled SFKM in the $T-U$ plane. Phase A, C, and D label the CDW phase, the uniform non-Fermi liquid metal, and the uniform insulator respectively.

can be shown[4] to diverge at the same temperature [for the same value of $X(\mathbf{q})$] as the b-charge-susceptibility discussed above. Therefore, a divergence of the b-charge-susceptibility [$\chi(\mathbf{q},T)$ in eq. (3.7)] also signals an instability towards the generation of long-range order in the ℓ charge density corresponding to the same parameter X.

The mapping $\mathbf{q}\rightarrow X(\mathbf{q})$ is a many-to-one mapping that determines an equivalence class of wave vectors in the Brillouin zone. In the $d\rightarrow\infty$ limit, "generic" wave vectors are all mapped to $X=0$, since $cosq_j$ can be thought of as a random number between -1 and 1 for generic points in the Brillouin zone. All the possible values of X ($-1\leq X\leq 1$) can be sampled, however, using a wave vector that lies on the diagonal of the first Brillouin zone extending from the zone center ($X=1$) to the zone corner ($X=-1$). An ordering at the zone corner [$X=-1,\mathbf{Q}=(\pi,\pi,...)$] corresponds to a two sublattice (checkerboard) state with the ℓ electrons preferentially occupying one sublattice [$exp(i\mathbf{Q}.R_j)=1$] and the b electrons preferentially occupying the other sublattice [$exp(i\mathbf{Q}.R_j)=-1$]. Here we only consider the $X=-1$ case. The susceptibility $\chi(\mathbf{q},T)$ then diverges at the temperature T_c ($X=-1$) and T_c as a function of U for the SDOS case is shown in Fig. 1. Phase C denotes the non-Fermi liquid metal ($\Im\Sigma(\omega=0)\neq 0$ and temperature independent), D is the uniform insulator and A is the two-sublattice or checkerboard charge-density-wave(CDW) phase[14].

IV. SPECTRAL AND TRANSPORT PROPERTIES OF THE CHARGE-DENSITY-WAVE PHASE

The checkerboard charge-density-wave(CDW) phase has two inequivalent sublattices, A and B, defined by:

$$\begin{aligned} exp(i\mathbf{Q}\cdot R_i) &= +1 \quad \text{for i belonging to A} \\ exp(i\mathbf{Q}\cdot R_i) &= -1 \quad \text{for i belonging to B} \end{aligned} \tag{4.1}$$

with $\mathbf{Q}=(\pi,\pi,\pi,.....)$. The two sublattices spontaneously develop different electronic densities relative to each other, but all sites of a given sublattice are equivalent. All the quantities such as w_{1i}, Σ_n^{ii}, G_n^{ii}, etc., introduced earlier in the DMFT formalism section now become double valued with respect to i. Hence we can write

$$\mathrm{w}_{1i}=\begin{cases}\mathrm{w}_{1a} & \text{if } i \text{ belongs to sublattice } A\\ \mathrm{w}_{1b} & \text{if } i \text{ belongs to sublattice } B\end{cases}. \tag{4.2}$$

Similarly, for the local self-energy and Green's function, one has

$$\Sigma_n^{ii}=\begin{cases}\Sigma_n^{A} & \text{if } i \text{ belongs to sublattice } A\\ \Sigma_n^{B} & \text{if } i \text{ belongs to sublattice } B\end{cases}; \tag{4.3}$$

$$G_n^{ii}=\begin{cases}G_n^{A} & \text{if } i \text{ belongs to sublattice } A\\ G_n^{B} & \text{if } i \text{ belongs to sublattice } B\end{cases}. \tag{4.4}$$

At half filling, by symmetry,

$$(\mathrm{w}_{1a}-\frac{1}{2})=-(\mathrm{w}_{1b}-\frac{1}{2})\equiv\Delta\mathrm{w}. \tag{4.5}$$

Hence, the relation eq. (2.9) becomes

$$\Sigma_n^{A,B}=\frac{U}{2}-\frac{1}{2G_n^{A,B}}\left(1-\sqrt{1+(UG_n^{A,B})^2\pm 4(\Delta\mathrm{w})UG_n^{A,B}}\right), \tag{4.6}$$

To complete the DMFT self consistency loop, we have to solve the lattice Dyson equation eq. (2.13) in the present, two sublattice CDW context. For this purpose it is convenient to introduce a two-component spinor field $\psi_{\mathbf{k}}$,

$$\psi_{\mathbf{k}}\equiv\begin{pmatrix}b_{\mathbf{k}A}\\ b_{\mathbf{k}B}\end{pmatrix}, \tag{4.7}$$

with

$$b_{\mathbf{k}A}\equiv\sum_{i\epsilon A}b_i\exp(i\mathbf{k}.\mathbf{R}_i)\ ,$$

etc., where $\mathbf{k}$ now only takes values within the reduced Brillouin zone corresponding to the A sublattice alone. In terms of the matrix Green's function defined in the usual way as

$$\mathbf{G}_{\mathbf{k}n}\equiv<<\psi_{\mathbf{k}};\psi_{\mathbf{k}}^{\dagger}>>\ , \tag{4.8}$$

the lattice Dyson equation eq. (2.13) reduces in the present context to the simple 2 x 2 matrix equation

$$[(i\omega_n + \mu)\mathbf{1} - \mathbf{M}_{\mathbf{k}n}]\mathbf{G}_{\mathbf{k}n} = \mathbf{1}, \tag{4.9}$$

where

$$\mathbf{M}_{\mathbf{k}n} = \begin{pmatrix} \Sigma_n^A & \epsilon_{\mathbf{k}} \\ \epsilon_{\mathbf{k}} & \Sigma_n^B \end{pmatrix}. \tag{4.10}$$

Hence $\mathbf{G}_{\mathbf{k}n}$ is given by

$$\mathbf{G}_{\mathbf{k}n} = \begin{pmatrix} \xi_n^A & -\epsilon_{\mathbf{k}} \\ -\epsilon_{\mathbf{k}} & \xi_n^B \end{pmatrix}^{-1}, \tag{4.11}$$

with

$$\xi_n^{A,B} \equiv i\omega_n + \mu - \Sigma_n^{A,B} \ .$$

The local Green's functions $G_n^{A,B}$ are just the diagonal components of the matrix:

$$\mathbf{G}_n = \sum_{\mathbf{k}} \mathbf{G}_{\mathbf{k}n}. \tag{4.12}$$

Hence we get, finally,

$$G_n^{A,B} = \xi_n^{B,A} \int \frac{D_0(\epsilon)d\epsilon}{\xi_n^A \xi_n^B - \epsilon^2} = \frac{G_0(z_n)}{z_n} \xi_n^{B,A}, \tag{4.13}$$

where $D_0(\epsilon)$ is bare DOS of the b band as before,

$$z_n \equiv \sqrt{\xi_n^A \xi_n^B} \ ,$$

and $G_0(z)$ is the complex Hilbert Transform of the bare DOS as defined before in eq. (3.11). Again, for the case of the semi-circular DOS the calculations become simpler as $G_0(z)$ is analytically known (cf eq. (3.5)).

We note that Δw can be thought of as the order parameter characterizing the CDW phase. In the uniform phase, Δw= 0, and $\Sigma_n^A = \Sigma_n^B$, etc., and all the above equations reduce to the corresponding equations discussed earlier for the uniform case.

V. RESULTS AND DISCUSSION

Next we discuss in detail our results for the DMFT spectral and transport properties in the CDW phase of the half-filled SFKM. For convenience we measure all energies such as ω, U, *etc.* in units of t for the SDOS, and $2t$ for the 2DDOS. Consequently, the bare b band width on the Bethe lattice or on the square lattice is $W = 4$.

The main result from our study is summarized in the *new 'phase diagram'* for the half-filled SFKM, shown in Fig. 2. As noted before in the introductory section, there is a region in the phase diagram, marked B in Fig. 2 and not emphasized in the literature before, where the CDW phase order parameter is non-zero, *but there is no gap in the spectrum.* This is unlike the Hartree-Fock (HF) mean-field theory prediction, where the CDW phase is always gapped. We will refer to this as the "gapless CDW phase". Furthermore, the 'transition temperature' $T_l(U)$ between this novel 'phase' and the conventional gapped CDW phase has an interesting *reentrant* structure as U increases, as depicted in Fig. 2.

This emerges from a study of results such as the ones shown in Fig.s 3-5. Fig. 3 shows the CDW order parameter (Δw) as a function of the temperature T for five values of $U = 0.5, 1.0, 1.5, 2.0, 2.5$. In Figs. 4 and 5 we have shown the evolution of the local spectral function for SDOS and 2DDOS[15] respectively as a function of temperature and U. In the uniform phase, the spectral functions are temperature independent as we have

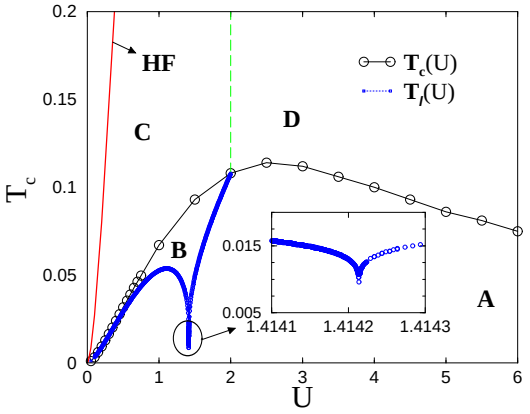

FIG. 2: (Color online) New phase diagram of the half-filled SFKM in the $T - U$ plane. Phase A, B, C, and D represent gapped CDW, gapless CDW, uniform non-Fermi liquid metal, and uniform insulator respectively.

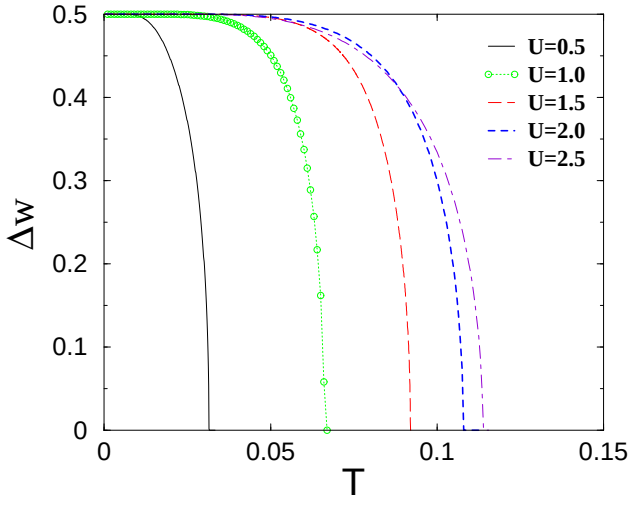

FIG. 3: (Color online) Variation of the order parameter (Δw) with temperature for different values of U. (All the energies are scaled in units of t.)

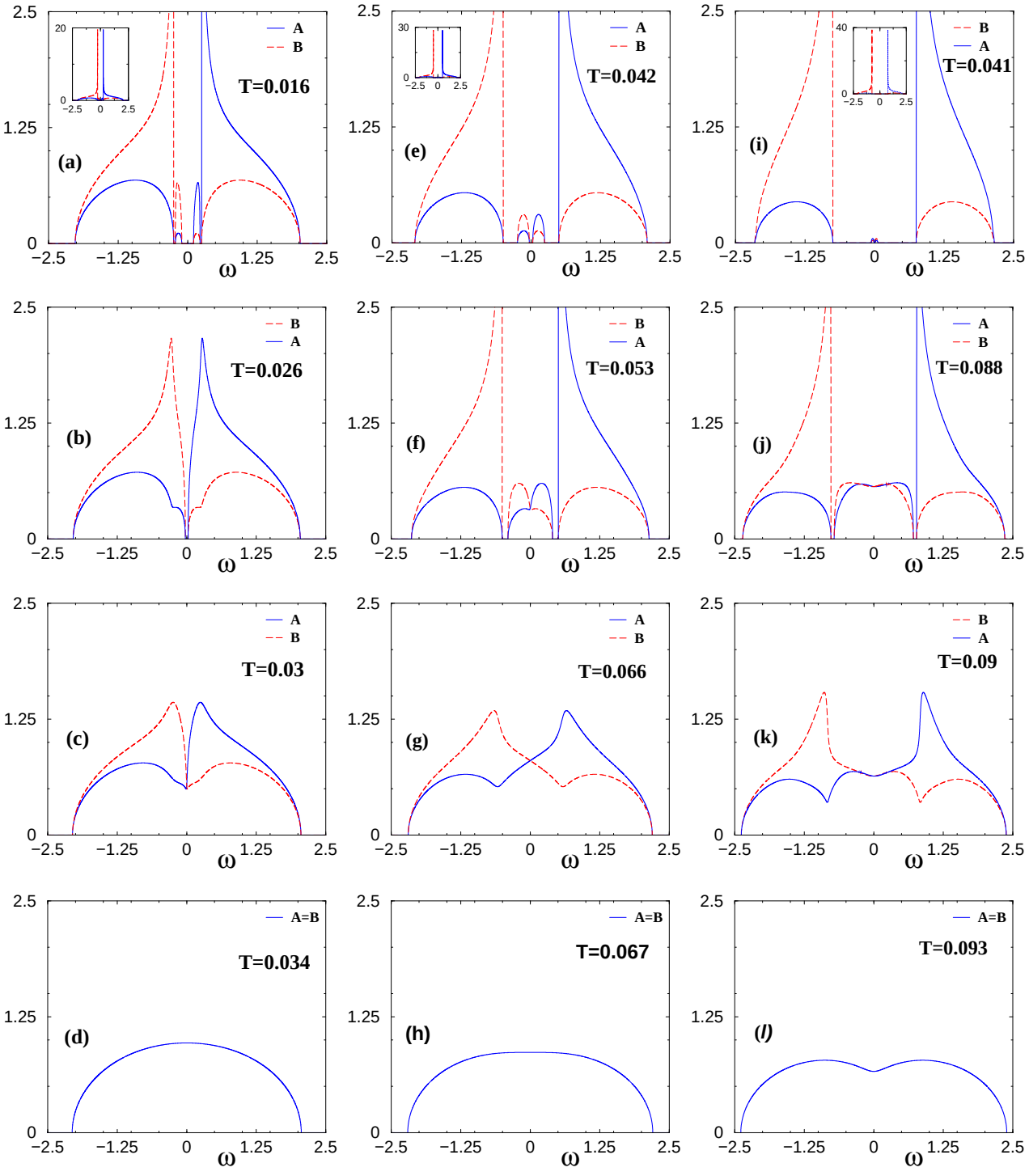

FIG. 4: (Color online) Diagrams showing the evolution of local spectral function for SDOS as a function of temperature for three values of $U = 0.5, 1.0, 1.5$ in the first, second, and third columns respectively, and in increasing order of temperature. Dotted lines are for sublattice A and long dashed lines are for sublattice B.

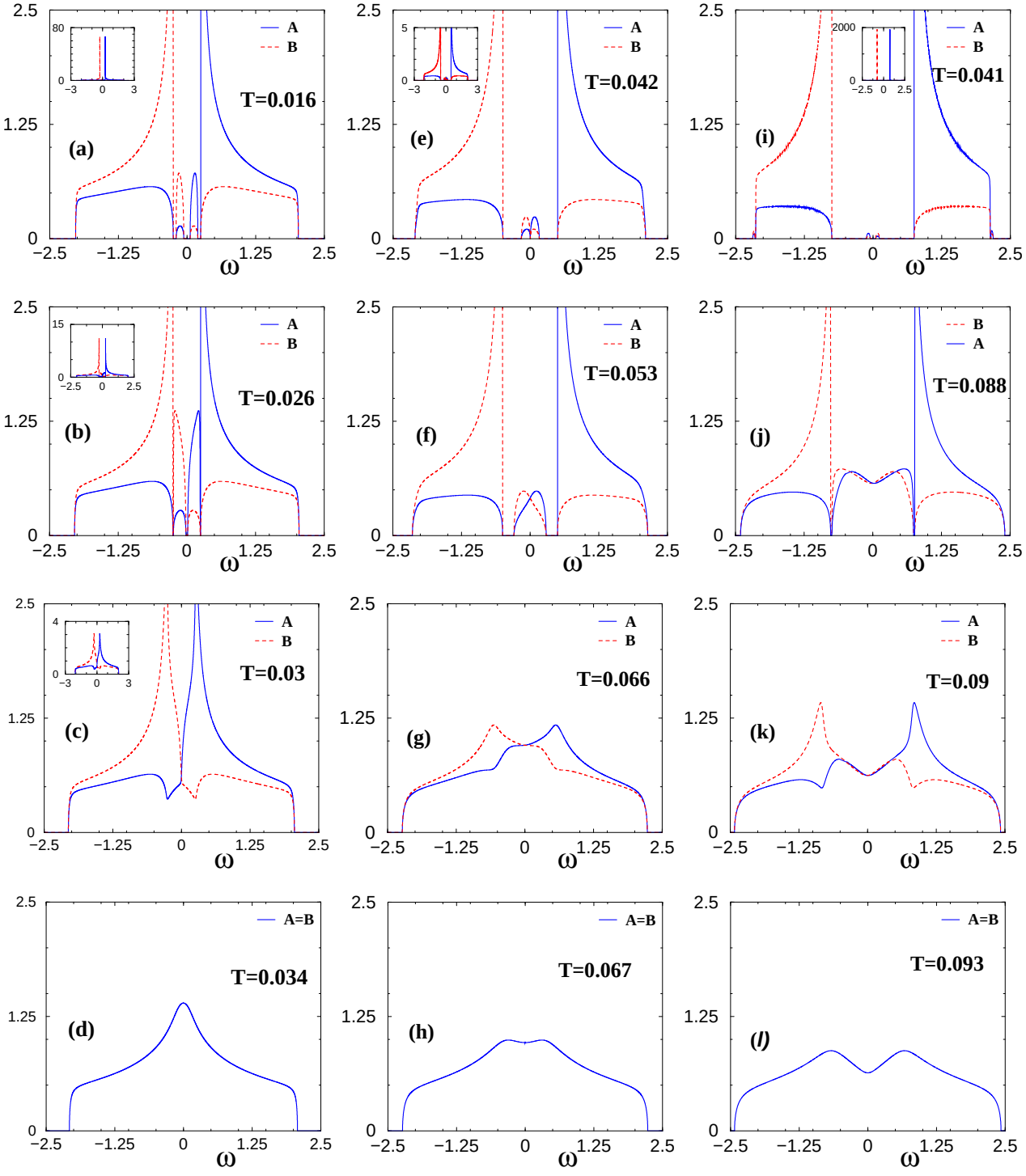

FIG. 5: (Color online) Diagrams showing the evolution of local spectral function for 2DDOS as function of temperature for three values of $U = 0.5, 1.0, 1.5$ in the first, second, and third columns respectively, and in increasing order of temperature. Dotted lines are for sublattice A and long dashed lines are for sublattice B.

remarked before, and their U dependence can be seen in the bottom panels of Fig. 4 for the SDOS case and in Fig. 5 for 2DDOS[15]. Basically, as U increases, there is a transfer of spectral weight from low frequencies out to large frequencies, leading to the formation of 'Hubbard bands' and a 'pseudo gap'. Eventually, for $U > U_{MI}$ ($U_{MI} = 2$ for SDOS) a real gap opens up, and a metal insulator transition ensues, as indicated in Fig. 2. As we decrease the temperature at a fixed U within the checker-board phase, there is spectral weight transfer from low frequencies to near a threshold frequency corresponding to the HF gap. However, as can be seen in the next (second from bottom) set of panels in Figs. 4 and 5, a real gap in the spectral function does not develop just after one crosses into the checker-board phase as would be predicted, for example, by the HF approximation. Rather it develops only below the lower critical temperature $T_l(U)$ shown in Fig. 2. Even more interestingly, $T_l(U)$ has a reentrant feature as function of U (see Fig. 2).

We note that at $T = 0$, Δw=0.5, $\Sigma_n^A = U$ and $\Sigma_n^B = 0$. The DMFT spectral functions at $T = 0$ are thus identical to the HF spectral functions, corresponding to split bands with dispersion $\pm\sqrt{(U/2)^2 + \epsilon_{\mathbf{k}}^2}$. The gap in the spectral function is hence exactly equal to U. However, as we increase the temperature the value of Δw deviates slightly from 0.5 and the spectral function for each sublattices develops two peaks around $\omega = 0$ and one observes three gaps as can be seen in the topmost panels in Figs. 4 and 5. As we increase the temperature further, these two peaks grow in intensity and the gaps away from $\omega = 0$ close up and only the gap around $\omega = 0$ remains. Eventually, past the lower critical temperature $T_l(U)$ mentioned above, even the gap around $\omega = 0$ vanishes, but the order parameter is still non-zero, until T crosses T_c whence Δw becomes zero and the local spectral function becomes uniform. This behavior is generic for $U < U_{MI}$. For $U > U_{MI}$, the spectrum is always gapped.

In the gapless CDW phase B, the b electrons are in a state which allows gapless excitations and coexist with ℓ electrons in a gapped state. We can view the effective ℓ electron energy as the centroid of the ℓ electron spectral function. The gap in ℓ electrons spectral function is therefore definable as $\epsilon^*_{\ell_A} - \epsilon^*_{\ell_B}$. The absence of a gap in the b-electron spectral function arises from the same source that causes the b-electrons in the uniform phase to acquire a non-Fermi liquid character, namely the ℓ-electrons which act as a source of disorder scattering, leading to a finite life time of the b electrons at the Fermi energy. In the CDW phase close to T_c and for U not too large, although there is long range staggered order in n_ℓ, there are large thermal fluctuations in n_ℓ which again act as disorder scatterers for the b-electrons, leading to a finite life-time at the Fermi surface and to a gapless b-electron spectral function. This feature goes away at low temperatures or for large U, as the order in n_ℓ gets stronger and the fluctuations get reduced.

To get a quantitative estimate of the lower critical temperature T_l, we have studied the quantity

$$\Gamma \equiv \Im\,(\Sigma_A + \Sigma_B)_{\omega=0}$$

as a function of temperature, as the vanishing of Γ signals the opening up of the gap around $\omega = 0$. Figs. 6 and 7 depict Γ as a function of temperature and Δw respectively for $U = 0.5, 1.5, 1.55, 1.75$. We note that at $U = 0.5$ the gap closes up at $T_l = 0.029$ (corresponding Δw=0.240). As we increase U the gap closes up at higher values of temperature, *i.e.*, at $T_l = 0.052$ (Δw=0.435) for $U = 1$. However, as we increase U further, the gap closes up at lower values of T_l up to U very close to $\sqrt{2}$ and $T_l = 0.0108$ (Δw$\simeq$ 0.5). Beyond $U \simeq \sqrt{2}$ the lower critical temperature T_l for the closing of the gap again increases to join the T_c versus U curves at $U = 2.0$. Hence we get the reentrant curve for T_l as shown in Fig. 2.

The lower critical temperature T_l shown in Fig. 2 was

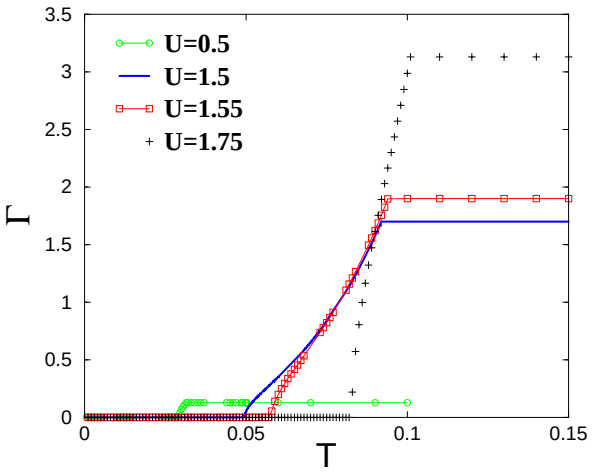

FIG. 6: (Color online)Variation of $\Gamma(\equiv \Im\,(\Sigma_A+\Sigma_B)$ at $\omega = 0$) with temperature for different values of U for SDOS.

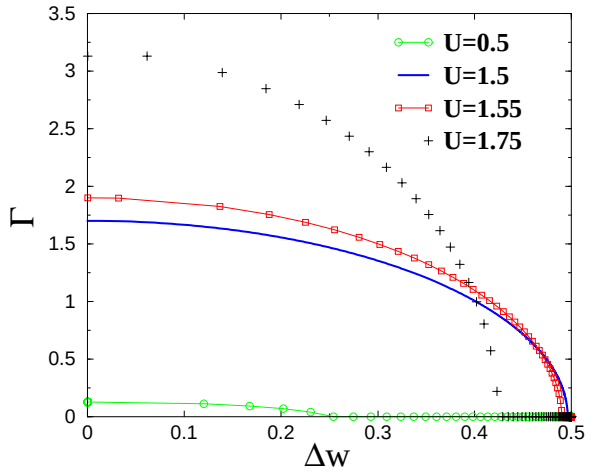

FIG. 7: (Color online)Variation of Γ with the order parameter (Δw) for different values of U for SDOS.

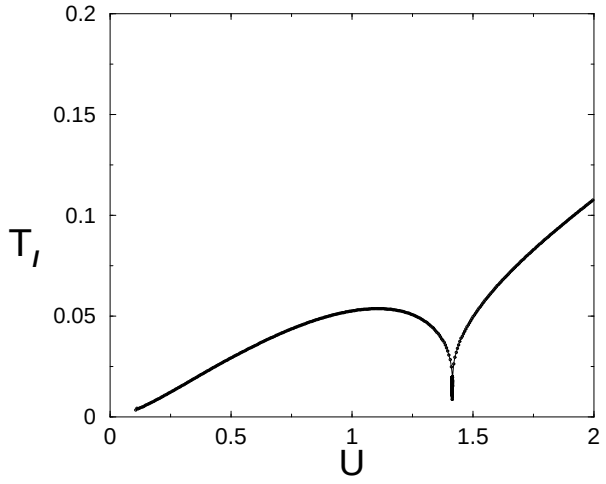

FIG. 8: Variation of the critical temperature T_l with U.

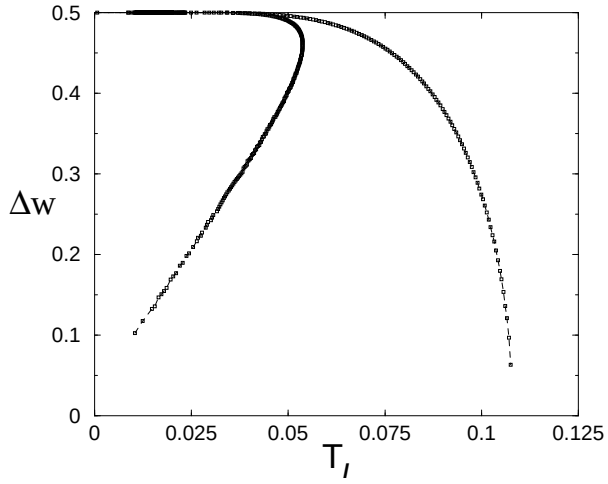

FIG. 9: Variation of the order parameter (Δw) with the critical temperature T_l.

obtained by analyzing the data of spectral functions and the order parameter as discussed above. Using the relation $\Sigma^A(\omega=0) = -(\Sigma^B(\omega=0))^*$ and the expression for $\Sigma^A(\omega=0)$ from eq. (4.6), and invoking the condition for the vanishing of Γ, we obtain the following implicit equation for T_l:

$$\Delta\mathrm{w}(T_l) + \frac{U}{2} Re(G^A(\omega=0;T_l)) = 0. \qquad (5.1)$$

$T_l(U)$ can be very accurately determined using eq. (5.1) and the results are exhibited in Fig.8, and in the inset of Fig.2. We have also computed the order parameter (Δw) as a function of T_l and U on the curve $T_l(U)$, and we have shown these in Figs.9 and 10. As we move along the curve $T_l(U)$ in Fig. 2 the order parameter (Δw) first increases, helped both by the increase of U and the decrease of T, approaching a maximum value very close to 0.5 at U$\simeq \sqrt{2}$. However, as we move to larger values of U, the order parameter (Δw) starts decreasing and vanishes at U=2.0, where T_l joins T_c.

When Δw is very close to 0.5, then Σ^A and Σ^B are very close to U and 0 respectively. Substituting these values in eqs. (4.13) and (5.1), we obtain

$$Re\{(G^A)^{-1}\} \simeq -\frac{\frac{U}{2} + \sqrt{(\frac{U}{2})^2 + 4t^2}}{2} \simeq -U. \qquad (5.2)$$

Solving eq. (5.2), we can verify that the dip of the lower critical temperature T_l occurs at $U \simeq \sqrt{2}$.

It is interesting to ask how these novel features in the spectral functions affect experimentally measurable quantities. In particular, we have studied the optical conductivity $\sigma(\omega)$ as a function of T and U. In the CDW phase it can be shown to be given by[16]

$$\sigma(\omega) \;=\; \pi\frac{e^2}{2\hbar a}\int_{-\infty}^{\infty} d\epsilon D_{tr}(\epsilon)\int_{-\infty}^{\infty}\frac{d\omega}{2\pi} Tr(\sigma^x \mathbf{A}(\epsilon,\omega')$$

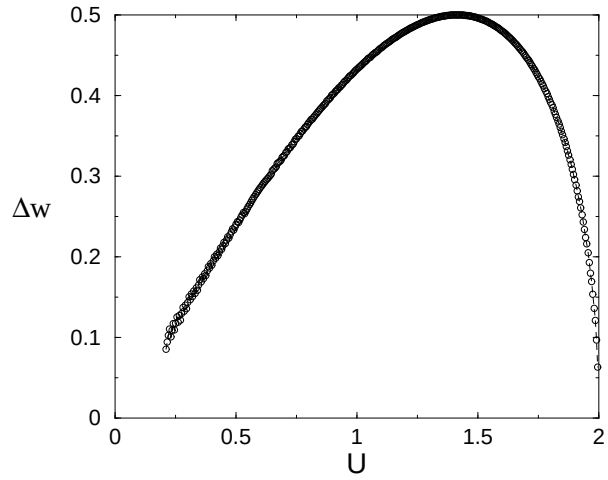

FIG. 10: Variation of the order parameter (Δw) with U on the curve T_l.

$$\times\sigma^x \mathbf{A}(\epsilon,\omega'+\omega))\frac{n_F^-(\omega') - n_F^-(\omega'+\omega)}{\omega}, \qquad (5.3)$$

where σ^x is the Pauli matrix, $\mathbf{A}(\epsilon,\omega') = -\frac{1}{\pi}\Im\mathbf{G}_\epsilon(\omega')$, is the matrix spectral function for the matrix Green's function given by eq. (4.11), and $D_{tr}(\epsilon)$ is the transport DOS[16,17]. We plot $\sigma(\omega)$ for different values of temperatures for a fixed value of $U = 0.5$ in Figs. 11 and 12 for the SDOS and 2DDOS respectively. When T=.016 one can see from the spectral function (first diagram of column 1 of Fig. 4) that the gap around $\omega = 0$ is roughly 0.25, and there are two bands of low spectral weights which are separated from the main bands by a second smaller gap (0.05) around $\omega = 0.5$. These features are reflected in $\sigma(\omega)$ (see Fig. 11 dot-dashed curve) which shows that there is no optical response up to $\omega = 0.25$. Then there is a rise, a small dip around $\omega = 0.5$, followed by a sharp peak. As we increase the temperature

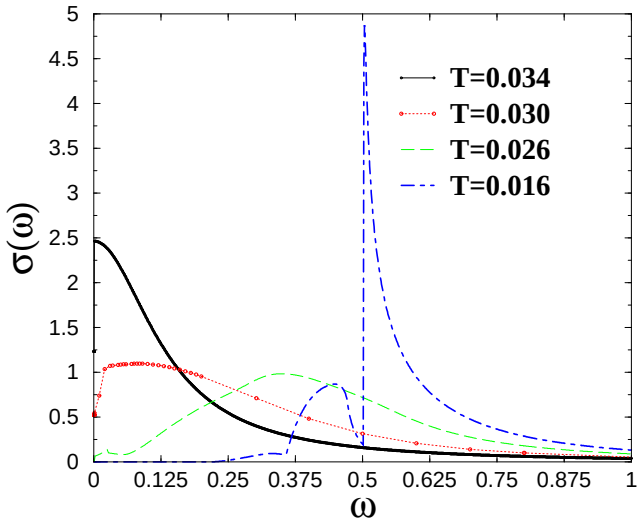

FIG. 11: (Color online) Optical Conductivity $\sigma(\omega)$ at different temperatures for a fixed value of $U = 0.5$ for SDOS

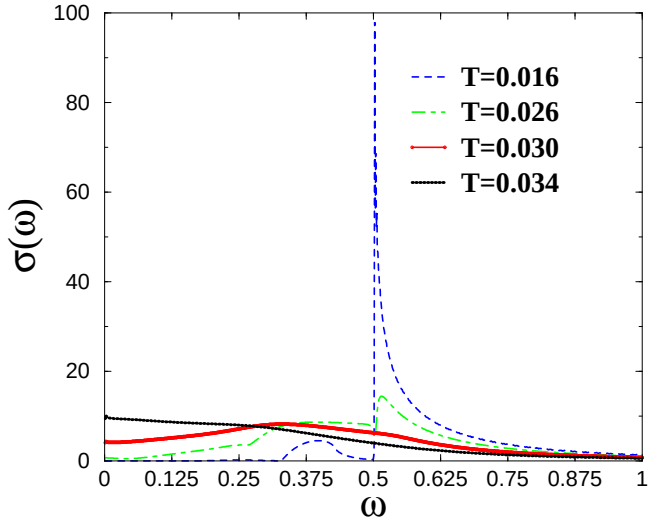

FIG. 12: (Color online) Optical Conductivity $\sigma(\omega)$ at different temperatures for a fixed value of $U = 0.5$ for 2DDOS

to $T = 0.026$ (see second diagram of column 2 of Fig. 4), the spectral function now has a very small gap around $\omega = 0$, this feature of spectral function is reflected in the corresponding $\sigma(\omega)$ (see Figs. 11(long dashed curve) and 12 (dot-dashed curve)). Similarly, the other two curves for the optical conductivity at $T = 0.03$ and $T = 0.032$ (Fig. 11 dotted and solid lines respectively) correspond to the spectral functions in the last two diagrams of column 1 in Fig. 4. We note however that the dc conductivity $\sigma(\omega = 0)$ does not capture these features, and reflects only the transition from the CDW to the uniform phase which shows up as a slope discontinuity at T_c, as can be seen in Fig. 13.

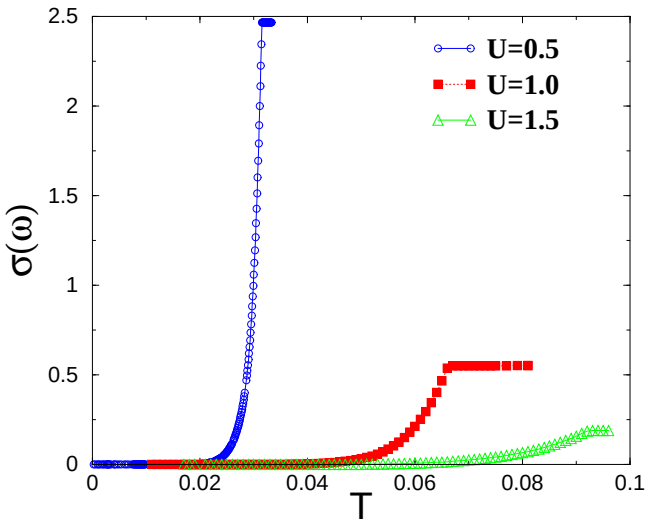

FIG. 13: (Color online)dc-conductivity as a function of temperature for a fixed value of $U = 0.5$, 1.0, 1.5.

VI. CONCLUDING DISCUSSION

In conclusion, we have presented results from a detailed DMFT study of the spectral functions in the CDW phase of the half-filled SFKM as function of temperature and U. We have shown that the proximity of the non-Fermi liquid metallic phase affects the CDW phase, leading to a region in the phase diagram where we a get CDW phase *without a gap in the spectral function*. Interestingly, this gapless CDW phase shows a *reentrant transition* to the gapped CDW phase as U increases. This is a radical deviation from mean-field prediction where the CDW phase is always gapped, with the gap being proportional to the order parameter. We have also discussed how these features affect response functions, *e.g.*, the optical conductivity. It would be interesting to study whether, and to what extent these features survive when one goes beyond DMFT for the SFKM, *e.g.* in more sophisticated approximations such as the Dynamical Cluster Approximation[13,18], cluster-DMFT[19] or Variational Cluster Approximation[20], which include the effects of short range inter-site correlations.

We note that gapless CDW phases are easy to achieve even within the Hartree approximation by considering second neighbor hopping, which gets rid of nesting. What is novel about the gapless CDW phase discussed here is that it is correlation induced, and appears despite the presence of perfect nesting. It is interesting to ask whether such phases can appear in other models with strong correlations. The normal (repulsive) Hubbard model does not have CDW instabilities. But an extended Hubbard model with nearest neighbor repulsion V would. We believe that at intermediate values of the Hubbard U and appropriate values of V the extended Hubbard model with nearest neighbor hopping could exhibit a gapless

commensurate CDW phase. For, the DMFT treatment of such a model in the presence of a CDW would correspond closely with the recent study[21] of correlation effects in a two sublattice band insulator where correlations were shown to induce metallicity.

On the experimental front, gapless CDW phases have recently been observed in 2H- transition metal dichalcogenides (eg., ref. 22 and references therein). In these compounds, strongly coupled electronic and lattice degrees of freedom are involved in the generation of the CDW instability, and the gapless feature has been attributed to very large second neighbor hopping. Since in our model we are considering only electronic degrees of freedom, and only nearest neighbor hopping, we have not compared the experiments directly with our findings.

VII. ACKNOWLEDGMENTS

SRH thanks the Council of Scientific and Industrial Research(India) and NSERC (Canada) for financial support, and gratefully acknowledges useful discussion with G.Venkateshwara Pai and R. Karan. HRK's research was supported by the University Grants Commission (India), the Department of Science and Technology(India) and the Indo-French Centre for the Promotion of Advanced Research (grant no. 2400-1). He would also like to acknowledge the hospitality of the KITP (supported by NSF grant no. PHY05-51164) during the preparation of the revised manuscript.

---

* Also at the Jawaharlal Nehru Centre for Advanced Scientific Research, Jakkur, Bangalore 560 064, India.

[1] W. Metzner and D. Vollhardt, Phys. Rev. Lett., **62**, 324 (1989).

[2] Th. Pruschke, M. Jarrell and J. K. Freericks, Adv. Phys., **42** 187, (1995)

[3] A. Georges, G. Kotliar, W. Krauth, and M. J. Rozenberg, Rev. Mod. Phys., **68**, 1 (1996)

[4] U. Brandt and C. Mielsch, Z. Phys. B, **75**, 365 (1989); *ibid* **79**, 295 (1990); **82**, 37 (1991).

[5] L. M. Falicov and J. C. Kimball, Phys. Rev. Lett., **2**, 997, 1969

[6] T. Kennedy and E. H. Lieb, Physica, **138A**, 320 (1986).

[7] Q. Si, G. Kotliar and A. Georges Phys. Rev. B **46**, 1261 (1992).

[8] G. Moller, A. E. Ruckenstein and S. Schmitt-Rink Phys. Rev. B **46**, 7427 (1992).

[9] P. G . J. van Dongen and D. Vollhardt, Mod. Phys. Lett. B **5**, 861 (1991); P. G. J. van Dongen, Phys. Rev. B **45**, 2267 (1992).

[10] J. K. Freericks, Phys. Rev. B **47**, 9263 (1993a); *ibid* **48**, 14797 (1993b): J. K. Freericks, C. Gruber and N. Macris, *ibid* **60**, 1617(1999); J. K. Freericks and R. Lemanski, Phys. Rev. B **61**, 13438 (2000); J. K. Freericks and V. Zlatic, Rev. Mod. Phys **75**, 1333 (2003)

[11] C. Gruber, N. Macris, P. Royer, and J.K. Freericks, Phys. Rev. B **63**, 165111 (2001).

[12] B. M. Letfulov, Europhys. J. B **11**, 423 (1999).

[13] M. H. Hettler, A. N. Tahvildar-Zadeh, M. Jarrell, Th. Pruschke and H. R. Krishnamurthy, Phys. Rev. B **58**, R7475 (1998)

[14] The Bethe lattice is a connected cycle-free graph where each node is connected to Z neighbors, where Z is called the coordination number. This leads to a tree-like structure emanating from a central node (called the root or origin of the lattice), with all the nodes arranged in shells around the central one. The number of nodes in the kth shell is given by $N_k = Z(Z-1)^{(k-1)}$ for $k > 0$. A checkerboard phase on the Bethe lattice corresponds to placing b and ℓ electrons on alternating nodes.

[15] The results obtained from the DMFT of the SFKM in two dimensions (local approximation) are qualitatively similar to the results of infinite-dimensional hypercubic lattice (reference no 10,1993b). Small quantitative differences arise only because of the different DOS appropriate to the two cases. We note in addition that the local approximation is asymptotically exact at weak coupling. Deviations from the exact answer for the 2-d case are also expected only to be quantitative, and sizable only in strong-coupling limit (where the model maps onto on effective Ising model at half filling), eg., a reduction in T_c due to spatial fluctuation that are neglected in the local approximation. These deviation can be reduced, for example, by considering spatial fluctuation within DCA[13].

[16] Th. Pruschke, D. L. Cox and M. Jarrell, Phys. Rev. B **47**, 3553 (1993).

[17] For the hypercubic lattice, $D_{tr}(\epsilon)=\frac{1}{N}\sum_{\mathbf{k}} v_{k_x}^2 \delta(\epsilon-\epsilon_{\mathbf{k}})$. In the infinite-dimensionality limit, it is proportional to the bare DOS[16]. For the purpose of this paper we have set $D_{tr}(\epsilon)=D_0(\epsilon)$ given by eqn. (8).

[18] M. H. Hettler, M. Mukherjee, M. Jarrell, and H. R. Krishnamurthy, Phys. Rev. B **61**, 12739 (2000); T.Maier, M. Jarrell, T. Pruschke and M. H. Hettler, Rev. Mod. Phys. **77**, 1027 (2005)

[19] G. Kotliar, S. Y. Savrasov, G. Palsson and G. Biroli, Phys. Rev. Lett. **87**, 186401 (2001).

[20] M. Potthoff, Eur. Phys. J. B **36**, 335 (2003)

[21] Arti Garg, H. R. Krishnamurthy, and Mohit Randeria, Phys. Rev. Lett. **97**, 046403 (2006).

[22] R. L. Barnett, A. Polkovnikov, E. Demler, W. G. Yin, W. Ku, Phys. Rev. Lett. **96**, 026406 (2006).

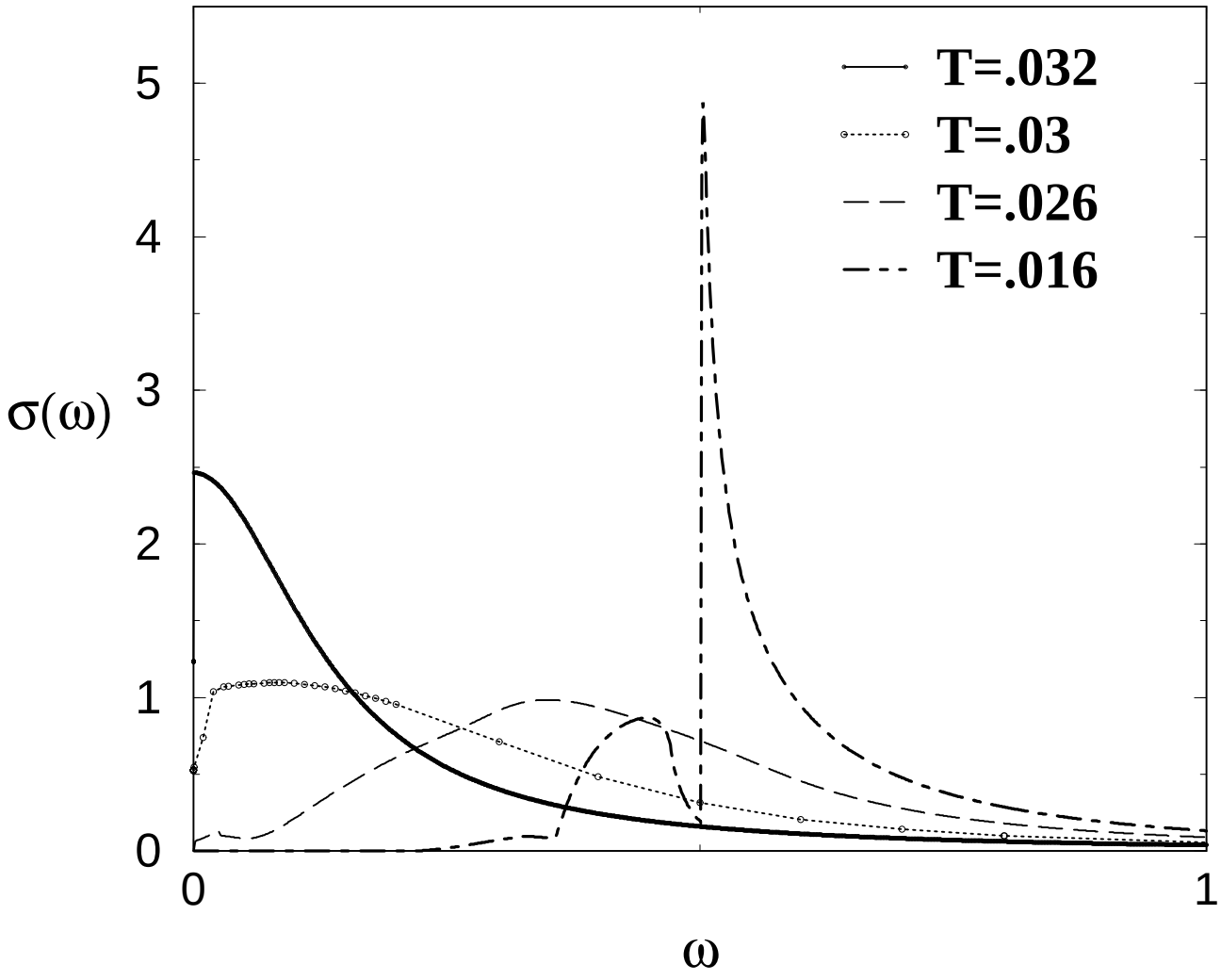
T=.032
T=.03
T=.026
T=.016
σ(ω)
ω
0
1
2
3
4
5
0
1

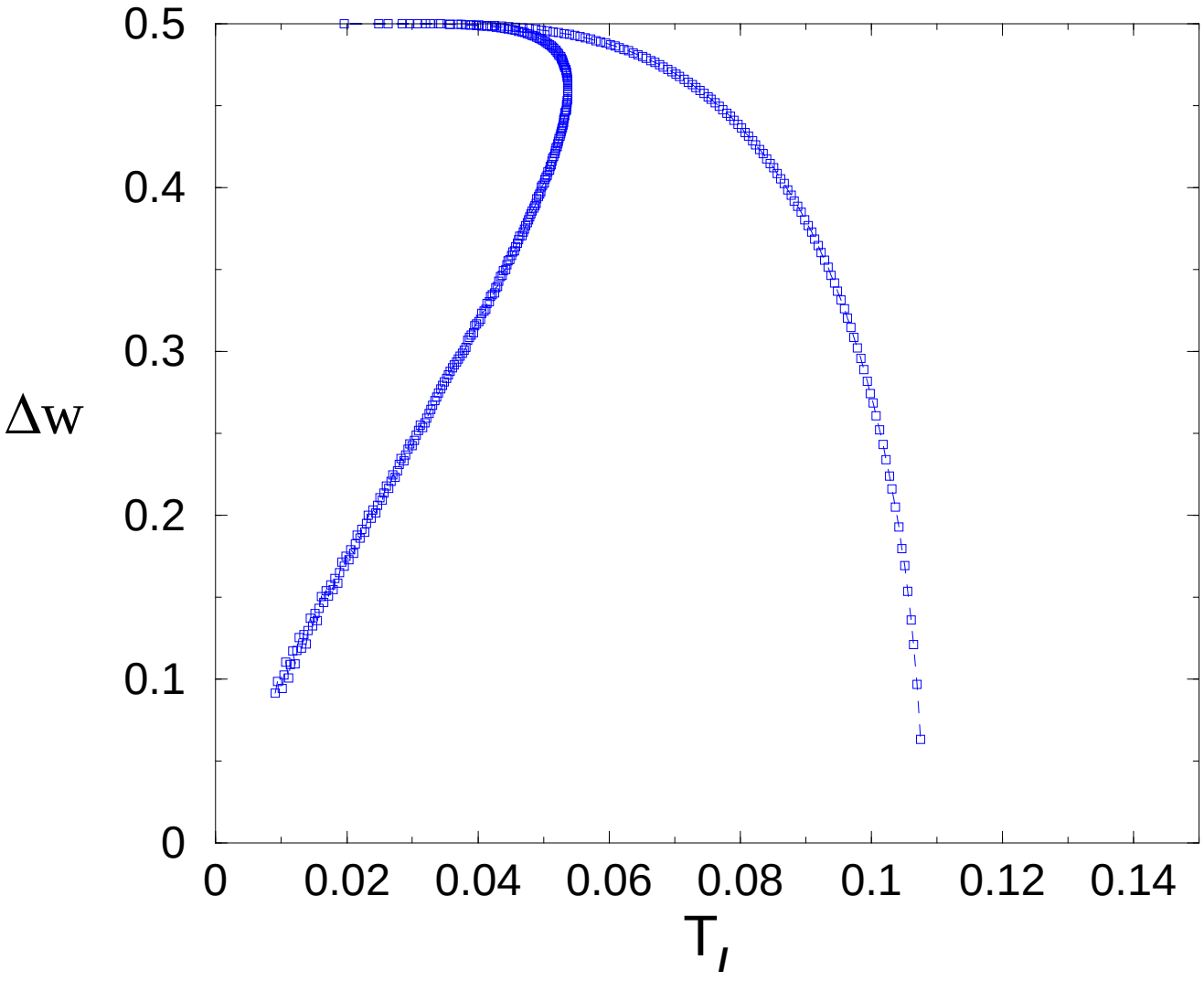
0.5
0.4
0.3
0.2
0.1
0
Δw
0
0.02
0.04
0.06
0.08
0.1
0.12
0.14
T_I